Research Article

Nano Biomed Eng

Potassium Dichromate Detection: Carbon Quantum Dot-based Fluorescent "Turn-Off" Nanoprobe Design

Priti Sharma[1], Sopan Nangare[1], Rahul Tade[1], Pravin Patil[1], Sanjkumar Bari[1], Dipak Patil[2]✉

[1] Department of Pharmaceutical Chemistry and Quality Assurance, H. R. Patel Institute of Pharmaceutical Education and Research, Shirpur 425405, Dhule (MS), India

[2] Department of Pharmaceutical Chemistry, K. K. Wagh College of Pharmacy, Hirabai Haridas Vidyanagari, Amrutdham, Panchavati, Nashik 422 003, Nashik (MS), India

✉ Corresponding author. E-mail: dipakpatil888@gmail.com

Received: Dec. 2, 2023; **Revised:** Jan. 12, 2024; **Accepted:** Feb. 5, 2024

Citation: P. Sharma, S. Nangare, R. Tade, et al. Potassium dichromate detection: carbon quantum dot-based fluorescent "turn-off" nanoprobe design. *Nano Biomedicine and Engineering*, 2024.

http://doi.org/10.26599/NBE.2024.9290069

Abstract

The occurrence of potassium dichromate in food poses serious health risks, including cancer and skin-related issues. Conventional sensing methods, known for their poor sensitivity, low selectivity, and high costs, highlight the need for improved detection methods. This study addresses this gap by exploring the use of carbon quantum dots (CQDs) synthesized from *Tamarindus indica* leaves through an eco-friendly hydrothermal approach for the detection of potassium dichromate. Briefly, the synthesized CQDs underwent spectroscopic characterizations. Following this, the CQDs-based sensor was assessed for key analytical parameters such as sensitivity, selectivity, and the analysis of spiked milk samples to detect potassium dichromate. As a result, analyses of particle size and zeta potential confirmed the formation of stable, nanosized CQDs. The introduction of potassium dichromate led to the quenching of CQDs' fluorescence, likely attributed to mechanisms such as the inner filter effect (IFE) and fluorescence resonance energy transfer (FRET). The established linearity range and limit of detection were determined to be 50–500 and 148 μmol/L, respectively. Confirmation of the sensor's practicality was obtained through the analysis of spiked samples, suggesting that CQDs could potentially serve as a viable alternative for detecting potassium dichromate in milk samples in the future.

Keywords: Carbon quantum dots; potassium dichromate; fluorescence; biomedical sensor; nanoprobe

Introduction

From its inception, harmful practices have often been employed in milk preparation, dilution, and other purposes. Among these practices, the addition of water to increase the quantity or volume is the most common scenario in the milk industry. According to existing literature, milk adulteration is considered one of the most intricate forms of fraud within the entire industry. Specifically, the addition of melamine to milk, following water dilution, substantially elevates nitrogen levels [1]. To extend the shelf life of products, additional ingredients, such as formaldehyde, hydrogen peroxide, hypochlorite,

dichromate, and salicylic acid, have been reported to be used. Additionally, the fat content is adulterated using vegetable oils or surfactants, while the protein content is manipulated through the use of cheese whey and urea [2, 3]. Despite these various foreign materials, one notable milk stabilizer is potassium dichromate. However, potassium dichromate can lead to adverse effects such as skin irritation, rhinitis, and allergic contact dermatitis. Furthermore, it serves as a potent biocide that can contribute to sewage problems and increased levels of chromium in drinking water [4]. In addition, studies have shown that potassium dichromate is a known carcinogen, capable of causing cancer in humans [5]. A literature survey has reported that when mothers consume significant amounts of chocolate and cocoa, which are rich sources of chromium, it can lead to hypersensitivity in their infants [6]. To date, different sensors have been documented for the detection of potassium dichromate. In brief, the nanomaterials-based fluorescent sensor [7, 8], colorimetric sensor [9], etc. have been documented. Despite this development, the detection with improved sensitivity is a major challenge. Overall, there is an urgent need for the development of effective methods to detect potassium dichromate in milk samples.

For the detection of milk adulterants, several spectroscopical and advanced analytical techniques have been accounted. Particularly, it includes differential scanning calorimetry (DSC), reversed-phase-high-performance liquid chromatography (RP-HPLC), high-performance thin layer chromatography (HPTLC), Fourier-transform infrared spectroscopy (FTIR), capillary electrophoresis (CE), the fluorescence of advanced Maillard products and soluble tryptophan (FAMPST), enzyme-linked immunosorbent assay (ELISA), near-infrared (NIR) spectroscopy, sodium dodecyl sulfate-polyacrylamide gel electrophoresis (SDS-PAGE) based approaches, etc. [10]. Despite several merits of the mentioned methods, there are major limitations including a tedious process, high cost, poor sensitivity, low selectivity, etc. that restrict their application in the detection of adulterants in milk samples. Hence, there is a need to search for sensitive, selective, cost-effective, rapid, and simplistic, etc. methods that can overcome the limitations of the conventionally reported methods.

Since their inception, carbon dots (CDs) or carbon quantum dots (CQDs) have been among the most extensively studied carbon-based nanoparticles [11]. Importantly, CQDs are zero-dimensional carbon-based nanomaterials [12, 13]. According to the literature, CQDs represent a fascinating type of carbon nanostructure with an approximate diameter of 10 nm [14]. It can be synthesized using top-down and bottom-up methods from different sources, natural or synthetic [15]. They possess exceptional and distinctive properties. The reported studies have confirmed the high sensitivity, selectivity, good stability, and practicality of the method [16]. It has been widely applied in various biomedical fields, such as sensing [17] and drug delivery [18]. To date, CQDs and their modified versions have been documented for the design of nanosystems for electrocatalytic degradation [19], detection of biomarkers [20], pesticide detection [21], etc. Therefore, the application of CQDs for the detection of potassium dichromate promises to usher in a new era of food safety.

The objective of this study is to detect potassium dichromate in milk samples using CQDs as a fluorescent nanoprobe. To summarize, CQDs were synthesized from *Tamarindus indica* through the hydrothermal method and subjected to spectroscopic characterizations. Subsequently, the detection of potassium dichromate was conducted employing these CQDs. Furthermore, an anti-interference study was carried out to confirm the high selectivity of the proposed CQDs for potassium dichromate, even in the presence of various interfering molecules. Moreover, spiked sample analysis validated the real-time applicability of this method in milk samples. Therefore, looking ahead, the utilization of green-synthesized CQDs holds the potential to revolutionize the detection of potassium dichromate in milk samples.

Materials and Methods

Materials

Dry tamarind leaves were purchased from the local market in Shirpur (Dhule), India. Potassium dichromate ($K_2Cr_2O_7$, purity: 99%) was purchased from Merck Specialties Pvt. Ltd., Mumbai, India. Other metal salts and chemicals used in this work including ammonium sulfate ($(NH_4)_2SO_4$), sucrose ($C1_2H_{22}O_{11}$), sodium chloride (NaCl), mercuric

chloride ($HgCl_2$), boric acid (H_3BO_3), sodium hydroxide (NaOH), benzoic acid ($C_7H_6O_2$), salicylic acid ($C_7H_6O_3$), sodium carbonate (Na_2CO_3), sodium bicarbonate ($NaHCO_3$), glucose ($C_6H_{12}O_6$), urea (NH_2CONH_2), starch $(C_6H_{10}O_5)_n$, hydrochloric acid (HCl), sulphuric acid (H_2SO_4), quinine sulphate ($C_{40}H_{50}N_4O_8S$) were collected from Loba Chemie Pvt. Ltd., Mumbai, India. All chemicals of analytical grade used in the experiment were analytical grade and were utilized without additional processing. The double distilled water (DDW) of HPLC grade (0.45 μm filtered) was used during experimentation.

Green synthesis of CQDs

The green synthesis of CQD was performed via hydrothermal method with dry tamarind (*Tamarindus indica*) [22]. The dried leaves of tamarind were washed with DDW several times and scorched at 70 °C in a hot air oven for 30 min, and then crushed into fine powder. 5 g of the powder was mixed with 100 mL of DDW using a magnetic stirrer for 20 min. Finally, the obtained mixture was transferred to the Teflon-lined stainless steel autoclave for the synthesis of CQDs. During this process, the temperature of the hot air oven was kept at 160 °C for 8 h. After the reaction, the obtained brown solution was centrifuged for 15 min at 12 000 r/min using a laboratory cold centrifuge. Finally, a 0.22 μm membrane filter was used to separate the undissolved materials from CQDs. The supernatant solution of CQDs was purified for 24 h using a dialysis bag (10K molecular-weight cutoffs (MWCO)). The dialyzed CQDs were kept at 4 °C for further characterizations and applications.

Characterizations

Ultraviolet–visible (UV–Vis) spectroscopy (UV spectrophotometer 1800 Shimadzu, Japan) was used to ensure the synthesis of CQDs from a green precursor. FTIR (IR-Affinity-1, Shimadzu, Japan) was used to confirm the functionality present on the surface of CQDs. The X-ray Diffractogram (XRD) of CQDs was validated using Versa Probe III (Physical Electronics, IIT Roorkee, India). The particle size analysis, poly-dispersity index, and zeta potentials of CQDs were also examined utilizing a dynamic light scattering-based particle size analyzer (NanoPlus3 Particulate System, Micrometrics, USA). The particle size and shape analysis and pattern of CQDs were assured using high-resolution transmission electron microscopy (HR-TEM, JEOL/JEM2100) including a selected area electron diffraction (SAED) facility operating at 200 kV. The surface binding energy of CQDs was confirmed using X-ray photoelectron spectroscopy (XPS, Versa Probe III, Physical Electronics). The fluorescence analysis was performed using a laboratory UV cabinet (Southern Scientific Lab Instrument, Chennai, India). A spectrofluorometer (JASCO International Co., Ltd., Japan) was used to accomplish the sensing of potassium dichromate in the provided samples.

Fluorescence study

At first, the obtained dispersion of CQDs was checked in a UV cabinet for fluorescence analysis at different wavelengths, such as 254, 365 nm, and visible light. After that, the CQDs emission spectra were recorded at various excitation wavelengths (350–440 nm) to achieve the high emission peak with proper Gaussian [23]. In addition, excitation spectra and emission spectra of the CQDs were reported using a spectrofluorometer for further study.

pH stability of CQDs

The effect of pH on fluorescence stability was validated using different pH solutions. Initially, the stock solution of CQDs (10 mg/100 mL) in double distilled water (DDW) was produced. After that, the pH of the CQDs solution was adjusted and confirmed using a laboratory digital pH meter (Equiptronics). After 30 min, the effect of pH on the fluorescence behavior of CQDs was examined with pH of 1–13 using a spectrofluorometer [22].

Quantum yield (QY) measurement

A QY of CQDs was calculated utilizing a standardized procedure considering quinine sulfate in 0.1 mol/L H_2SO_4 (literature QY: 0.54 at 360 nm) as the reference substance [24]. Absolute values are determined using the reference standards sample, which has a constant and well-known fluorescence QY value. To minimize the impact of the re-absorption, the absorbencies in the 10 mm fluorescent cuvette have been kept under 0.1 at the excitation wavelength of 360 nm. Finally, at an excitation wavelength of 360 nm, the QY of the CQDs was calculated using the following equation:

$$Q = Q_{st}\frac{A_{st}}{A} \times \frac{I}{I_{st}} \times \frac{n^2}{n_{st}^2}$$

where Q stands for quantum yield, I for emission intensity, n for solvent refractive index (RI), and A for

absorbance. The subscript "st" stands for the reference. The QY was found to be 15.4%.

Sensitivity study

A sensitivity study of pure potassium dichromate with known concentration was performed using green synthesized CQDs as a fluorescent nanoprobe. In brief, the different CQD probes (10 mg/100 mL) were prepared in separate test tubes using DDW for the analysis of the linearity range of potassium dichromate. Here, different concentrations of 10–500 µmol/L (10, 50, 100, 150, 200, 250, 300, 350, 400, 450, 500 µmol/L) of potassium dichromate were prepared using DDW. After that, the first concentration of potassium dichromate (10 µmol/L) was incorporated into the CQDs probe (10 mg/100 mL). After 15 min, the fluorescence intensity of the sample was measured using a spectrofluorometer at a 400 nm excitation wavelength. Here, the quenching of CQDs fluorescence with a correlation of concentration of potassium dichromate was observed at an emission wavelength of 500 nm using a spectrofluorometer. Next, the same procedure was repeated for the remaining samples of potassium dichromate. Each analysis was repeated in triplicates. The linearity range and calibration curve were calculated based on the concentration of potassium dichromate and quenched fluorescence of CQDs. Finally, the limit of detection (LOD) for potassium dichromate was calculated using a slope that was obtained from fluorescence repose against a concentration of potassium dichromate.

Selectivity study and pre-treatment of the milk samples

In this step, the specificity of the CQDs-based fluorescent probe was calculated. In short, different interfering agents such as ammonium sulfate, sucrose, potassium dichromate, sodium chloride, mercuric chloride, boric acid, sodium hydroxide, benzoic acid, salicylic acid, sodium carbonate, sodium bicarbonate, glucose, sodium saccharine, urea, and starch were selected for the selectivity study. At first, the stocksolution of CQDs (10 mg/100 mL) was prepared in DDW. After that, the 500 µmol/L concentration of each interfering substance was prepared in a separate test tube. Then 100 µL of this solution with different interfering milk adulterant substances was added to 2 mL of CQDs stock solution. Finally, the solution was diluted up to 3 mL with DDW. The change in fluorescence intensity was recorded under the excitation wavelength at 400 nm using the above-mentioned parameters. After that, the spiked samples analysis of potassium dichromate was performed in milk samples. In brief, to eliminate the proteins, milk samples were processed with trichloroacetic acid which was purchased from nearby supermarkets. Here, a centrifuge tube was filled with milk samples, and 1% (v/v) trichloroacetic acid solution and then subjected to sonication for 15 min. After this, the supernatant was filtered through a 0.22 µmol/L membranetoremoveparticulatesafterbeingcentrifugedat 12 000 r/mim for 15 min. Before performing fluorescence tests, the pH was neutralized with NaOH, and the filtrate was kept at 4 °C away from light. Finally, the concentration of the analyte was measured using quenched fluorescence of CQDs. The percent relative standard deviation was calculated to confirm the practical applicability of the anticipated sensor.

Results and Discussion

In this work, tamarind leaves were carbonized using a simple and affordable hydrothermal procedure to create CQDs.

Characterization of CQDs

UV cabinet analysis and UV–Vis spectroscopy

The aqueous solution of the CQDs shows light brown under normal light while it emits blue-colored fluorescence under UV light, which can be seen with an naked eye (Fig. 1(a)). In the case of 254 nm, it shows the blue color fluorescence for GQDs (Fig. 1(b)). The UV–Vis spectra of CQDs are depicted in Fig. 1(c). Here, a peak of around 279 and 335 nm is attributed to the $\pi \rightarrow \pi^*$ transition of C=C and the $n \rightarrow \pi^*$ transition of the C=O bond, respectively. It assured the successful conversion of the green precursor to graphitic nanomaterials that contain carboxylic functionality [25].

Zeta potential and FTIR analysis

Zeta potential analysis provides information related to the surface functionality of nanomaterials and their stability in the provided medium. In this work, the zeta potential for the CQDs' aqueous dispersion was obtained to be –11.93 mV (Fig. 2(a)), indicating the presence of highly concentrated negatively charged

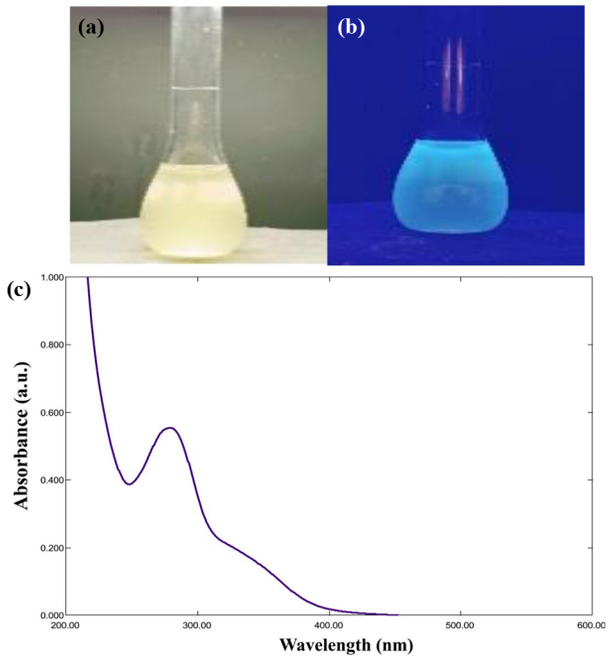

Fig. 1 (a) CQDs in normal light; **(b)** CQDs in UV light and **(c)** UV–Vis absorption spectra of green synthesized CQDs.

carboxylic groups on their surface. Overall, it confirmed that the green synthesized CQDs were stable in an aqueous system [26]. To assure surface functionality, the FTIR analysis was performed. Figure 2(b) demonstrates a very high absorption band at 3 300 cm^{-1}, which is attributed to O–H from stretching vibrations of the hydroxyl groups [27]. Another prominent absorption band at 1 650 cm^{-1} is caused by the C=O stretching vibration [28]. Hence, it confirmed the presence of carboxylic functionality on the surface of CQDs.

XPS analysis

The surface functionality of CQDs was validated using XPS analysis that provides the binding energy for carboxylic functionality, and amine functionality. In brief, the XPS survey scan spectrum of CQDs (Fig. 3(a)) indicates the presence of three peaks at 282.10, 397.59, and 530.07 eV attributed to characteristic peaks of carbon (C1s), nitrogen (N1s), and oxygen (O1s), accordingly. Figure 3(b) shows the C1s XPS spectrum. It is fitted into sp^2 and sp^3 hybridized carbon atoms in C–C/C=C at 282.12 eV, C–N/C–O at 284.46 eV, C=O/C=N at 289.81 eV, and O–C=O at 292.63 eV. Figure 3(c) shows the N1s XPS spectrum of CQDs, which presents the peak appearing at 394.12 eV corresponds to a C=N–C and 397.86 eV at C–N–C. The O1s XPS spectrum (Fig. 3(d)) of CQDs displays that the characteristic peaks at 529.15 and 532.16 eV correspond to the C=O bond

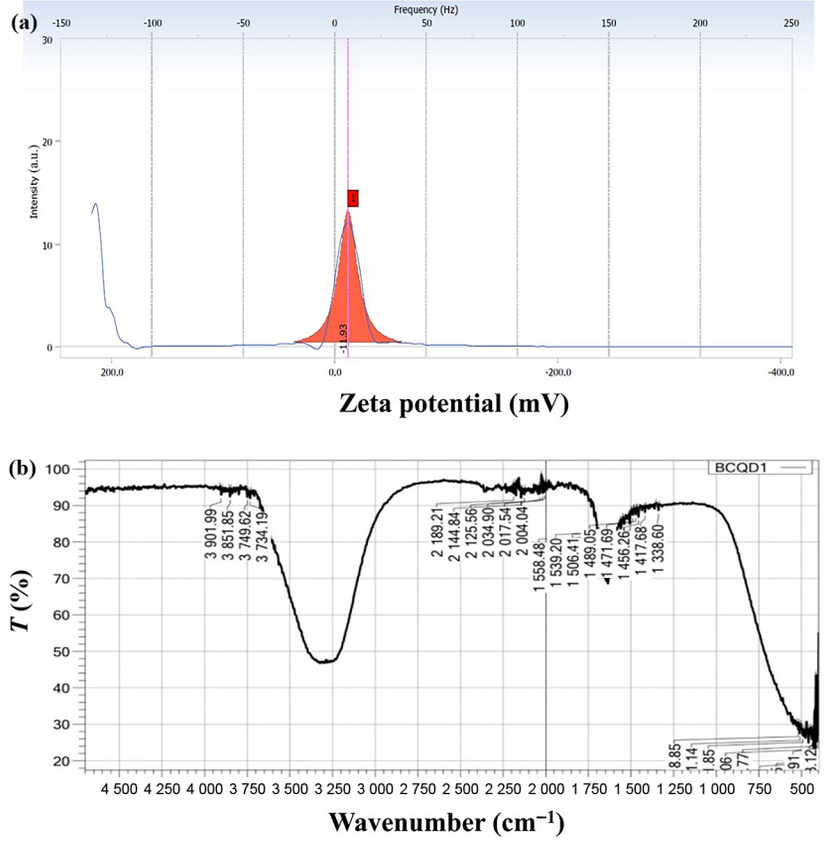

Fig. 2 (a) Zeta potential and **(b)** FTIR analysis of green-made CQDs.

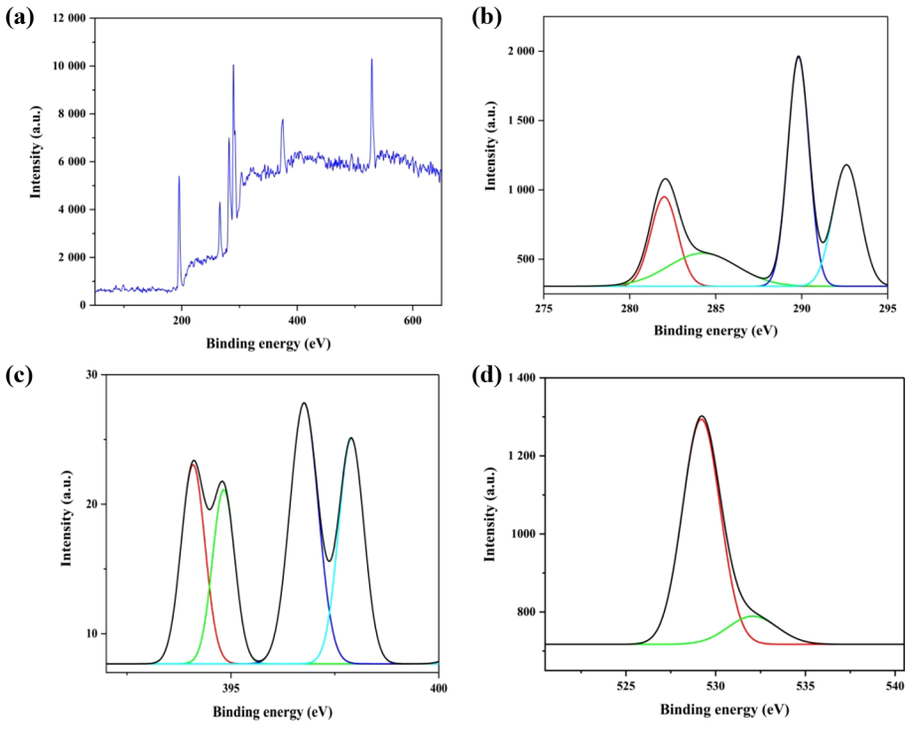

Fig. 3 (a) XPS spectrum of CQDs; **(b)** high-resolution spectrum of carbon (C1s); **(c)** high-resolution spectrum of nitrogen (N1s); **(d)** high-resolution spectrum of oxygen (O1s).

and the C–O–C bond, respectively. Taken as a whole, the synthesis of GQDs with plentiful carboxylic and amine functionality was found.

XRD and HR-TEM analysis

Figure 4 shows the X-ray diffractogram of synthesized CQDs from the green precursor. The peaks at 2θ = 28.53° and 40.33° correspond to the crystal planes of graphite carbon. Hence, it assured the synthesis of CQDs from tamarind leaves [29]. Figs. 5(a) and 5(b) provide insights into the surface morphology of CQDs, the particle size of CQDs, and their distribution. In brief, the resulting CQDs were homogeneous monodisperse with a mean range diameter of 5.1 nm. The shape of CQDs was obtained to be spherical whereas the SAED pattern (Fig.5(c)) reveals the polycrystalline nature of CQDs [30].

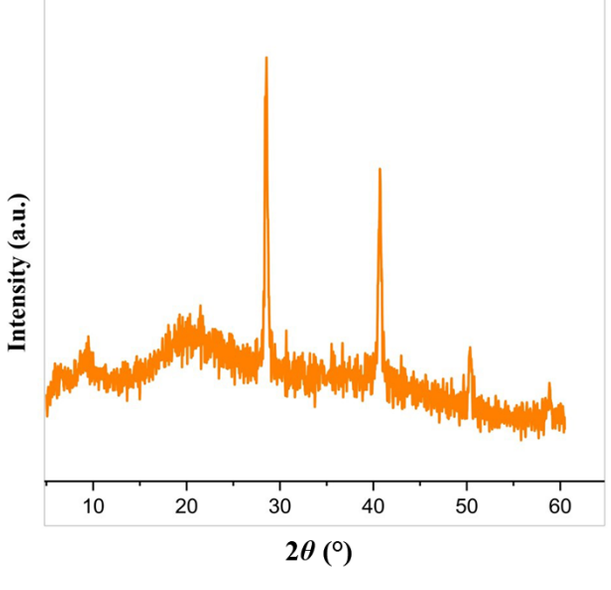

Fig. 4 Diffractogram of green-made CQDs.

Photoluminescence study and effect of pH

From an application standpoint, photoluminescence (PL) behavior is regarded as the most important attribute and is the traditional trademark of CQDs. The fluorescence emission spectrum of CQDs was examined at various excitation wavelengths with a constant 10 nm range between 350 and 450 nm. The tunable emissive character of CQDs is amply proven by their emission spectra, which are shown in Figs. 6(a) and 6(b). It was discovered that there was a red shift in emission wavelengths, which is known to be a characteristic of graphitic carbon cores [31]. In this study, the impact of pH on the CQDs' fluorescence intensity throughout a broad pH range of 3–13 was investigated. In brief, at a lower pH (3–5), the fluorescence intensity of CQDs was comparatively low, suggesting the existence of certain acidic groups on their surface. In contrast, CQD fluorescence was nearly constant in the solution with a pH range of 5–13 (Fig. 6(c)). The observed quenching of CQDs fluorescence in different pH may

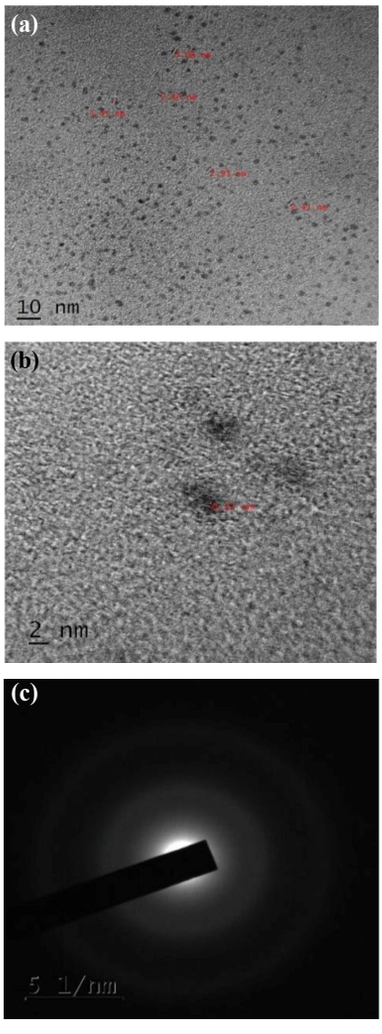

Fig. 5 (a, b) HR-TEM images and **(c)** SAED pattern of CQDs.

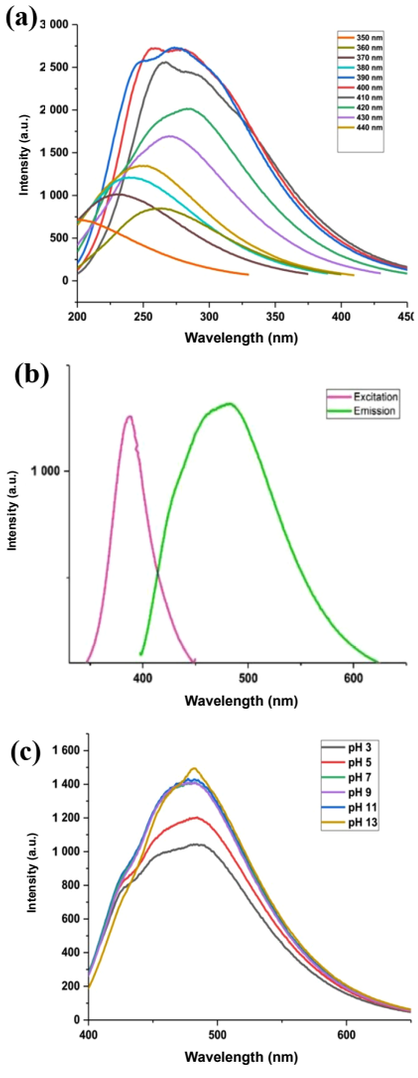

Fig. 6 (a) CQDs emission spectra at various excitation wavelengths. (b) Excitation, and emission spectra of CQDs. (c) The effect of pH from 3–13 on photoluminescence properties of CQDs.

be influenced by the protonation state of CQDs containing functional groups, highlighting the critical role of this factor in fluorescence intensity [32]. Impressively, the CQDs exhibited considerable stability in the aqueous phase across a broad pH range of 5–13. This noteworthy stability enhances their potential utility across various industries.

Sensitivity, selectivity, and spiked sample analysis of potassium dichromate using CQDs

The change in fluorescence property of CQDs was checked after the addition of potassium dichromate. At first, a series of fluorescence emission spectra at an excitation wavelength was recorded at 400 nm. The addition of potassium dichromate in concentrations ranging from 50 to 500 μmol/L into CQDs shows a decrease in fluorescence. As a result, with a rise in the content of potassium dichromate, the luminescence of the CQDs solution is steadily reduced. The fluorescence quenching of CQDs may occur upon the addition of potassium dichromate, involving various theoretical mechanisms, including energy transfer or electron transfer mechanisms. In this context, potassium dichromate acts as a potent oxidizing agent capable of accepting electrons from CQDs containing functional groups. This electron transfer can induce changes in the electronic structure of the CQDs, ultimately affecting their ability to emit fluorescence. Consequently, the fluorescence of CQDs may be quenched following the addition of potassium dichromate. Additionally, an energy transfer process from the excited state of CQDs to dichromate ions may contribute to fluorescence quenching, a phenomenon known as Förster resonance energy transfer. It's important to note that the alteration of the electronic structure of CQDs is a key factor in the observed fluorescence quenching

after the introduction of potassium dichromate. Based on this, the quenching efficiency with potassium dichromate concentration was calculated, which shows an extraordinary linear relationship between them (Fig. 7(a)). The $y = mx + c$ was found to be $-3.95x + 2\ 073$ with $R^2 = 0.999$. The calibration plot of fluorescence intensity change of CQDs vs. potassium dichromate concentration is shown in Fig.7(b). Finally, the limit of detection (LOD) for potassium dichromate was found to be 148 μmol/L whereas limit of quantitation (LOQ) was determined to be 450 μmol/L. In this study, the possible mechanism for the detection of potassium dichromate was due to spectral overlap between the CQDs and potassium dichromate.

In the case of common interference, the selectivity of the present sensors to potassium dichromate was studied. Remarkably, a significant quenching in fluorescence intensity was observed due to potassium dichromate addition. Possibly, this is due to energy transfer between the potassium dichromate and oxygen functional groups on the surface of the CQDs to form chelate complexes. As an effect, it leads to strong quenching of the CQD luminescence (Fig. 7(c)). The amounts of potassium dichromate in various milk samples were also determined using the provided probe. The recoveries of potassium dichromate in milk samples ranged from 96.22% ± 1.24% to 98.92% ± 1.29%, as shown in Table 1. There are no relative standard deviations (RSD) greater than 5% ($n = 3$). These outcomes showed that the anticipated probe has acceptable repeatability and good precision. As a result, the current method has the potential to be used in real-world situations to identify potassium dichromate in materials.

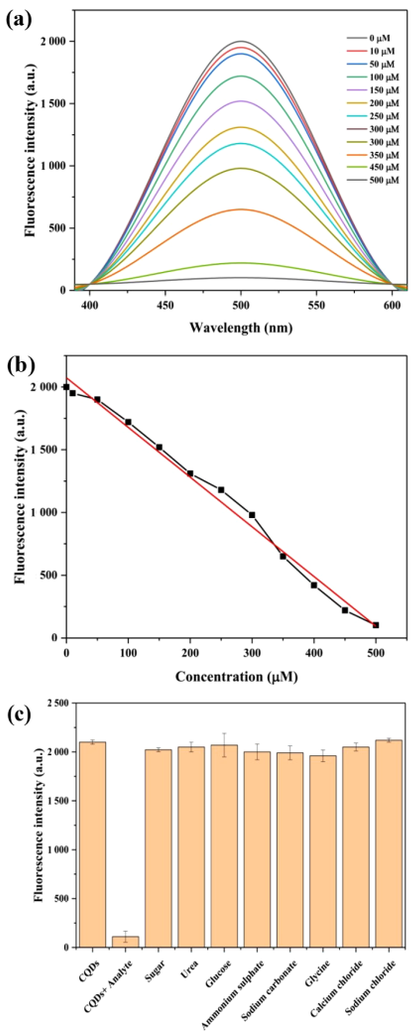

Fig. 7 (a) PL emission spectra of CQDs with altered concentrations of potassium dichromate (10–500 μmol/L). **(b)** Calibration plot of fluorescence intensity change of CQDs vs. potassium dichromate concentration. **(c)** Test of selectivity of CQDs for potassium dichromate in the presence of different interfering agents.

Table 1 Determination of potassium dichromate in milk samples

Milk Sample ($n = 3$)	Spiked concentration (μmol/L)	Percent recovery (%)	RSD (%)
1	300	97.24 ± 2.19	2.19 ± 0.89
	400	98.92 ± 1.29	2.39 ± 2.11
	500	97.22 ± 2.87	3.25 ± 1.18
2	300	98.22 ± 1.02	1.27 ± 0.99
	400	97.88 ± 1.09	2.63 ± 0.65
	500	97.69 ± 1.88	2.45 ± 0.11
3	300	96.22 ± 1.24	2.62 ± 1.28
	400	97.22 ± 2.14	2.94 ± 1.49
	500	96.25 ± 2.52	1.29 ± 1.87

Conclusion

The current research showcases the utilization of tamarind leaves as a carbon source for the facile generation of CQDs through an eco-friendly hydrothermal process. These CQDs were successfully employed for detecting potassium dichromate in milk samples. The study revealed that the synthesized CQDs displayed distinct photoluminescence dependent on the excitation wavelength. Spectroscopic analysis confirmed the production of stable, nanosized, and pure CQDs from a green precursor, showcasing favorable binding energy. The

detection of potassium dichromate using these CQDs achieved a LOD at levels up to μmol/L concentrations. Furthermore, the sensor exhibited a broad linear range for potassium dichromate detection and showcased high selectivity even in the presence of various interfering substances. Consequently, the proposed CQDs-mediated fluorescent sensor ensures both high sensitivity and selectivity. The potential sensing mechanism underlying the detection involves a fluorescent "turn-off", attributed to spectral overlap between the analyte and CQDs. Finally, the validation of the proposed CQDs through the analysis of spiked potassium dichromate samples in milk underscores the practical applicability of this eco-friendly approach. In summary, CQDs produced using green methods demonstrate exceptional capabilities in detecting potassium dichromate in milk samples.

CRediT Author Statement

Priti Sharma: study conception and design, data collection, data analysis and interpretation of results, manuscript writing, and correction in manuscript. **Sopan Nangare, Rahul Tade and Pravin Patil:** data analysis and interpretation of results, manuscript correction. **Dipak D. Patil:** study conception and design, project supervision, data collection, data analysis and interpretation of results data curation, manuscript writing – review & editing, communication.

Acknowledgements

The authors express their gratitude to the H. R. Patel Institute of Pharmaceutical Education and Research, Shirpur, for providing the necessary facilities. Additionally, the authors would like to extend their thanks to IIT Roorkee for granting access to the XPS analysis facility. Sopan Nangare would like to acknowledge the Indian Council of Medical Research (ICMR), New Delhi, for providing the Research Associate (RA) fellowship.

Conflict of Interests

The authors affirm that they have no known financial or interpersonal conflicts that would have appeared to have an impact on the research presented in this study.

References

[1] Y. Lu, Y. Xia, G. Liu, et al. A review of methods for detecting melamine in food samples. *Critical Reviews in Analytical Chemistry*, 2017, 47(1): 51−66. https://doi.org/10.1080/10408347.2016.1176889

[2] A. Borin, M.F. Ferrão, C. Mello, et al. Least-squares support vector machines and near infrared spectroscopy for quantification of common adulterants in powdered milk. *Analytica Chimica Acta*, 2006, 579(1): 25−32. https://doi.org/10.1016/j.aca.2006.07.008

[3] J.W. Qin, K.L. Chao, M.S. Kim. Simultaneous detection of multiple adulterants in dry milk using macro-scale Raman chemical imaging. *Food Chemistry*, 2013, 138(2-3): 998−1007. https://doi.org/10.1016/j.foodchem.2012.10.115

[4] M. Kroger. Milk sample preservation. *Journal of Dairy Science*, 1985, 68(3): 783−787. https://doi.org/10.3168/jds.S0022-0302(85)80889-4

[5] J.A. Bertrand. Influence of shipping container, preservative, and breed on analysis of milk components of shipped samples. *Journal of Dairy Science*, 1996, 79(1): 145−148. https://doi.org/10.3168/jds.S0022-0302(96)76346-4

[6] P. Singh, N. Gandhi. Milk preservatives and adulterants: processing, regulatory and safety issues. *Food Reviews International*, 2015, 31(3): 236−261. https://doi.org/10.1080/87559129.2014.994818

[7] Y. Wang, L. Cheng, Z.Y. Liu, et al. An ideal detector composed of two-dimensional Cd (II)–triazole frameworks for nitro-compound explosives and potassium dichromate. *Chemistry–A European Journal*, 2015, 21(40): 14171−14178. https://doi.org/10.1002/chem.201502167

[8] Y.-F. Zhu, W.-Q. Guan, F. Lin, et al. A new luminescent Zn(II) complex: selective sensing of $Cr_2O_7^{2-}$ and prevention activity against orthodontic root absorption by suppressing inflammatory response. *Journal of Fluorescence*, 2020, 30(5): 1233−1240. https://doi.org/10.1007/s10895-020-02597-w

[9] S. Kannaiyan, Easwaramoorthy, A. Gopal. Biogenic synthesized silver colloid for colorimetric sensing of dichromate ion and antidiabetic studies. *Research on Chemical Intermediates*, 2017, 43(5): 2693−2706. https://doi.org/10.1007/s11164-016-2789-z

[10] A. Poonia, A. Jha, R. Sharma, et al. Detection of adulteration in milk: A review. *International Journal of Dairy Technology*, 2017, 70(1): 23−42. https://doi.org/10.1111/1471-0307.12274

[11] Z.L. Peng, C.Y. Ji, Y.Q. Zhou, et al. Polyethylene glycol (PEG) derived carbon dots: Preparation and applications. *Applied Materials Today*, 2020, 20: 100677. https://doi.org/10.1016/j.apmt.2020.100677

[12] K.S. Raju, G.S. Das, K.M. Tripathi. Nitrogen-doped carbon quantum dots from biomass as a FRET-based sensing platform for the selective detection of H_2O_2 and aspartic acid. *RSC Sustainability*, 2024, 2(1): 223−232. https://doi.org/10.1039/D3SU00343D

[13] Y.R. Shang, T.X. Liu, G. Chen, et al. N,P co-doped carbon quantum dots bridge g-C_3N_4 and SnO_2: Accelerating charge transport in S-scheme heterojunction for enhanced photocatalytic hydrogen production. *Journal of Alloys and Compounds*, 2024, 971: 172667. https://doi.org/10.1016/j.jallcom.2023.172667

[14] U.A. Rani, L.Y. Ng, C.Y. Ng, et al. A review of carbon quantum dots and their applications in wastewater treatment. *Advances in Colloid and Interface Science*, 2020, 278: 102124. https://doi.org/10.1016/j.cis.2020.

102124
[15] F. Sher, I. Ziani, M. Smith, et al. Carbon quantum dots conjugated with metal hybrid nanoparticles as advanced electrocatalyst for energy applications–A review. *Coordination Chemistry Reviews*, 2024, 500: 215499. https://doi.org/10.1016/j.ccr.2023.215499
[16] W. Song, X. Zhai, J. Shi, et al. A ratiometric fluorescence amine sensor based on carbon quantum dot-loaded electrospun polyvinylidene fluoride film for visual monitoring of food freshness. *Food Chemistry*, 2024, 434: 137423. https://doi.org/10.1016/j.foodchem.2023.137423
[17] X. Xu, R. Ray, Y. Gu, et al. Electrophoretic analysis and purification of fluorescent single-walled carbon nanotube fragments. *Journal of the American Chemical Society*, 2004, 126(40): 12736−12737. https://doi.org/10.1021/ja040082h
[18] M.H. Karami, M. Abdouss. Recent advances of carbon quantum dots in tumor imaging. *Nanomedicine Journal*, 2024, 11(1): 13−35. https://doi.org/10.22038/NMJ.2023.73847.1798
[19] J. Zhang, J.L. Ren, F.J. Wang, et al. Zero-dimensional N-doped carbon quantum dots and palladium co-modified titanium electrodes enhance the electrocatalytic degradation of oxytetracycline hydrochloride. *Journal of Alloys and Compounds*, 2024, 971: 172776. https://doi.org/10.1016/j.jallcom.2023.172776
[20] S.L. Alaqel, M.A. Algarni, A. Alharbi, et al. Novel spectrofluorometric method utilizing functionalized carbon quantum dots for determining histamine levels in nasal secretions: Implications for allergic rhinitis. *Spectrochimica Acta Part A*, *Molecular and Biomolecular Spectroscopy*, 2024, 304: 123418. https://doi.org/10.1016/j.saa.2023.123418
[21] H. Mei, X.L. Zhu, Z.Q. Li, et al. Manganese dioxide nanosheet-modulated ratiometric fluoroprobe based on carbon quantum dots from okra for selective and sensitive dichlorvos detection in foods. *Food Chemistry*, 2024, 434: 137507. https://doi.org/10.1016/j.foodchem.2023.137507
[22] S. Nangare, S. Patil, K. Chaudhari, et al. Graphene quantum dots incorporated UiO-66-NH_2 based fluorescent nanocomposite for highly sensitive detection of quercetin. *Nano Biomedicine and Engineering*, 2023, 15(1): 1−13. https://doi.org/10.26599/NBE.2023.9290005
[23] S. Nangare, S. Patil, A. Patil, et al. Bovine serum albumin-derived poly-l-glutamic acid-functionalized graphene quantum dots embedded UiO-66-NH_2 MOFs as a fluorescence 'On-Off-On' magic gate for para-aminohippuric acid sensing. *Journal of Photochemistry and Photobiology A*: *Chemistry*, 2023, 438: 114532. https://doi.org/10.1016/j.jphotochem.2022.114532
[24] S. Nangare, S. Baviskar, A. Patil, et al. Design of "turn-off" fluorescent nanoprobe for highly sensitive detection of uric acid using green synthesized nitrogen-doped graphene quantum dots. *Acta Chimica Slovenica*, 2022, 69(2): 437−444. https://doi.org/10.17344/acsi.2022.7333
[25] P. Brachi. Synthesis of carbon dots (CDs) through the fluidized bed thermal treatment of residual biomass assisted by γ-alumina. *Applied Catalysis B*: *Environmental*, 2020, 263: 118361. https://doi.org/10.1016/j.apcatb.2019.118361
[26] Y. Yang, X. Xing, T. Zou, et al. A novel and sensitive ratiometric fluorescence assay for carbendazim based on N-doped carbon quantum dots and gold nanocluster nanohybrid. *Journal of Hazardous Materials*, 2020, 386: 121958. https://doi.org/10.1016/j.jhazmat.2019.121958
[27] D. Rodríguez-Padrón, M. Algarra, L.A.C. Tarelho, et al. Catalyzed microwave-assisted preparation of carbon quantum dots from lignocellulosic residues. *ACS Sustainable Chemistry & Engineering*, 2018, 6(6): 7200−7205. https://doi.org/10.1021/acssuschemeng.7b03848
[28] M. Miao, S. Zuo, Y. Zhao, et al. Selective oxidation rapidly decomposes biomass-based activated carbons into graphite-like crystallites. *Carbon*, 2018, 140: 504−507. https://doi.org/10.1016/j.carbon.2018.09.018
[29] S. Tajik, Z. Dourandish, K. Zhang, et al. Carbon and graphene quantum dots: A review on syntheses, characterization, biological and sensing applications for neurotransmitter determination. *RSC Advances*, 2020, 10(26): 15406−15429. https://doi.org/10.1039/d0ra00799d
[30] R. Atchudan, T.N. Jebakumar Immanuel Edison, M. Shanmugam, et al. Sustainable synthesis of carbon quantum dots from banana peel waste using hydrothermal process for *in vivo* bioimaging. *Physica E*: *Low-Dimensional Systems and Nanostructures*, 2021, 126: 114417. https://doi.org/10.1016/j.physe.2020.114417
[31] A. Tyagi, K.M. Tripathi, N. Singh, et al. Green synthesis of carbon quantum dots from lemon peel waste: applications in sensing and photocatalysis. *RSC Advances*, 2016, 6(76): 72423−72432. https://doi.org/10.1039/C6RA10488F
[32] S. Nangare, K. Chaudhari, P. Patil. Poly-L-lysine functionalized graphene quantum dots embedded zirconium metal–organic framework-based fluorescence switch on-off-on nanoprobe for highly sensitive and selective detection of taurine. *Journal of Photochemistry and Photobiology A*: *Chemistry*, 2024, 446: 115158. https://doi.org/10.1016/j.jphotochem.2023.115158